

Supporting Information

Synergistic CeO₂-HMOR Bicomponent Catalyst Enables Efficient Coproduction of Dimethyl Carbonate and Methyl Formate via CO₂-Methanol Coupling Assisted by 1,1,1-Trimethoxymethane Hydrolysis

Yongle Guo^a, Zhe Yang^a, Dehao Shi^a, Xiaowei Zhang^b, Yingjie Shao^a, Wenjie Duan^a,

Zhewen Ma^c and Junying Tian^{a,*},

^aSchool of Petrochemical Technology, Lanzhou University of Technology, Lanzhou, Gansu, 730050, China; Key Laboratory of Low Carbon Energy and Chemical Engineering of Gansu Province, Lanzhou, Gansu, 730050, China. jytian@lut.edu.cn

^bGansu Jindun Chemical Co., Ltd., No. 11, Guchengping, Donggang Street, Lanzhou, Gansu, 730030, China.

^c State Key Laboratory of Advanced Processing and Recycling of Nonferrous Metals & School of Materials Science and Engineering, Lanzhou University of Technology, Lanzhou, 730050, China

Corresponding author: jytian@lut.edu.cn

Table of Contents

1. Experimental

2. Supplementary Figures and Tables

3. References

Experimental

Materials: $\text{Ce}(\text{NO}_3)_3 \cdot 6 \text{H}_2\text{O}$ (99.5 wt.%) and 1,1,1-trimethoxymethane (TMM, 99.56% wt.%, anhydrous) were obtained from Shanghai Macklin Biochemical Technology Co., Ltd. Sodium hydroxide (96.0 wt.%, AR), anhydrous methanol (97.0 wt.%, AR) and n-propanol (99.5 wt.%) were obtained from Sinopharm Chemical Reagent Co., Ltd. HZSM-5 and H β zeolites were purchased from Tianjin Shenneng Technology Co., Ltd. HY and HMOR zeolites were purchased from Nankai University Catalyst Co., Ltd.

Catalysts preparation:

Nano-rod CeO_2 was prepared by co-precipitation method as previously reported^[1]. Typically, 12.42 g of $\text{Ce}(\text{NO}_3)_3 \cdot 6\text{H}_2\text{O}$ and 8.44 g of NaOH were dissolved in 20 mL and 15 mL of deionized water, respectively. The precipitate was formed by a full mixing of above two solutions, and added to a 100 mL Teflon-lined stainless steel autoclave and crystallized at 100 °C for 24 h. When it cooled down to room temperature, the product was separated by filtration, washed with deionized water and ethanol several times and dried at 100 °C for a night. Finally, nano-rod CeO_2 sample was obtained after calcination in the air at 600 °C for 4 h.

CeO₂-HMOR, CeO₂-HZSM-5, CeO₂-H β and CeO₂-HMOR bifunctional catalysts were prepared by a simple mixing of powder of CeO₂ and zeolites.

For comparison, CeO₂-HMOR bifunctional catalyst were prepared by grinding mixing for 30 minutes, and by incipient wetness impregnation with aqueous of Ce(NO₃)₃•6H₂O, respectively. In addition, CeO₂-HMOR bifunctional catalyst also was prepared by co-precipitation method that were similar to the method of nano-rod CeO₂, except for the addition of HMOR zeolite to the precipitate before it was added to the Teflon-lined stainless steel autoclave.

Catalysts characterization

HRTEM analysis was obtained with a JEOL JEM-2100 instrument. SEM experiments were carried out on a ZEISS Gemini SEM 300 instrument. XRD patterns were obtained on a Rigaku SmartLab SE with scanning speed of 5° min⁻¹ during 5-80 °. N₂ adsorption experiments were performed on a Microactive ASAP 2460 apparatus at -196 °C. Contact angle testings were operated on Chengdedingsheng JY-82C instrument. IR spectra were collected by Thermo Fisher Scientific Nicolet iS20 with KBr matrix after desorption at 100 °C for 12 h. Py-IR spectra were collected in the range of 1400–1700 cm⁻¹ using a Bruker Tensor 27 spectrometer in transmission mode after desorption at 150 °C and 350 °C. The amounts of acidic sites were investigated by NH₃ temperature programmed experiment (NH₃-TPD) on a Micromeritics AutoChem II 2920 instrument with a TCD. The 100 mg sample was placed in the reaction tube and pretreated in the flow of He for 60 min at 600 °C with a heating rate of 10 °C min⁻¹. After the temperature cooled to 100 °C, the 10% NH₃/He mixed gas

was introduced for 1 hour. Next, the samples were purified with He for 60 min. NH_3 desorption process was carried out in the temperature range of 100 to 600 °C at a ramping rate of 10 °C min⁻¹ in the He atmosphere.

The in-situ IR spectra were obtained using a Thermo Scientific Nicolet iS50 instrument in transmission mode. Prior to the tests, the self-supported wafer samples were treated in N_2 atmosphere at 200 °C for 30 min to thoroughly remove adsorbed impurities. After the temperature of in-situ chamber dropped to 50 °C, the mixed gas of CO_2 , methanol and TMM was continuously introduced for 30 minutes. During this process, methanol and TMM solution were first pumped into the vaporization furnace to complete vaporization and then introduced into the sample chamber. Afterwards, the inlet and outlet of the chamber were sealed, and then the background spectrum was obtained at 50 °C with 0.1 MPa. The in-situ spectra were collected while the sample temperature was increased from 50 °C to 70 °C, 90 °C, 100 °C, 110 °C, 130 °C, 140 °C and maintained 140 °C for 15 min and 30 min.

Computational Models and Methods

In this theoretical study, all geometric and energetic calculations were performed using density functional approximation as implemented in the CP2K package.^[1] The exchange-correction energies were calculated using the generalized-gradient approximated Perdew–Burke–Ernzerh functional (GGA-PBE).^[2,3] The dispersion interaction was calculated by using the empirical parameterized Grimme (D3) method.^[4] The **valence-shell electrons** ($1s^2$ for H, $2s^22p^2$ for C, $2s^22p^4$ for O, and $3s^23p^2$ for Si) are described using hybrid Gaussian and plane-wave (GPW) basis sets^[5]. Such basis sets are at level of triple- ζ valence plus polarization function (TZVP) with minimizing basis set superposition errors.^[6] The cutoff energy of 600

Rydberg of auxiliary plane wave basis sets were applied. Core-shell electrons of all elements were described using the Norm-conserving and separable Goedecker-Teter-Hutter (GTH) pseudopotentials.^[7] Transition states of elementary reaction were computed by using the climbing image nudged-elastic-band method (CI-NEB) with a convergence criterion of 0.05 eV/Å.^[8] The cluster model was constructed from MOR zeolite super cell within a box of sizes of 25x25x25 Angstroms. One proton was introduced into the model and binding on bridge O atom to simulate the real catalyst environment.

Catalytic performance measurement

The catalytic performance measurement was operated using a 50 mL stainless autoclave reactor (Anhui Kemi Instrument Co., Ltd). A certain of methanol, TMM and catalyst were added into reactor. The reactor was purged several times with CO₂ and pressurized up to 3.0 MPa, and then heated at 140 °C for 3h. After reaction, the reactor was cooled to room temperature and depressurized. The liquid products were verified by ¹H NMR spectroscopy (AVANCE NEO, 400 MHz, using DMSO-d₆) and detected by a gas chromatograph (FULI 9790 II) with RB-INNOWAX capillary column and FID detector. The 1-propanol was used as an internal standard. After the reaction of measurement, the CeO₂-HMOR bicomponent catalyst was recycled by centrifugation followed by absolute methanol washing third times under ultrasound for 10 min.

The product yield and space time yield were calculated as follow:

Based on methanol:

$$\text{DMC yield} = \frac{\text{Amount of DMC formed (mmol)} \times 2}{\text{Amount of MeOH added (mmol)}} \times 100 \% \quad (\text{Eq. 1})$$

$$\text{DME yield} = \frac{\text{Amount of DME formed (mmol)} \times 2}{\text{Amount of MeOH added (mmol)}} \times 100 \% \quad (\text{Eq. 2})$$

Based on TMM:

$$\text{DMC yield} = \frac{\text{Amount of DMC formed (mmol)}}{\text{Amount of TMM added (mmol)}} \times 100 \% \quad (\text{Eq. 3})$$

$$\text{DME yield} = \frac{\text{Amount of DME formed (mmol)}}{\text{Amount of TMM added (mmol)}} \times 100 \% \quad (\text{Eq. 4})$$

$$\text{MF yield} = \frac{\text{Amount of MF formed (mmol)}}{\text{Amount of TMM added (mmol)}} \times 100 \% \quad (\text{Eq. 5})$$

$$\text{DMC formation rate} = \frac{\text{Amount of DMC formed (mmol)}}{\text{Amount of CeO}_2 \text{ added (g)}} \quad (\text{Eq.6})$$

Supplementary Figures and Tables

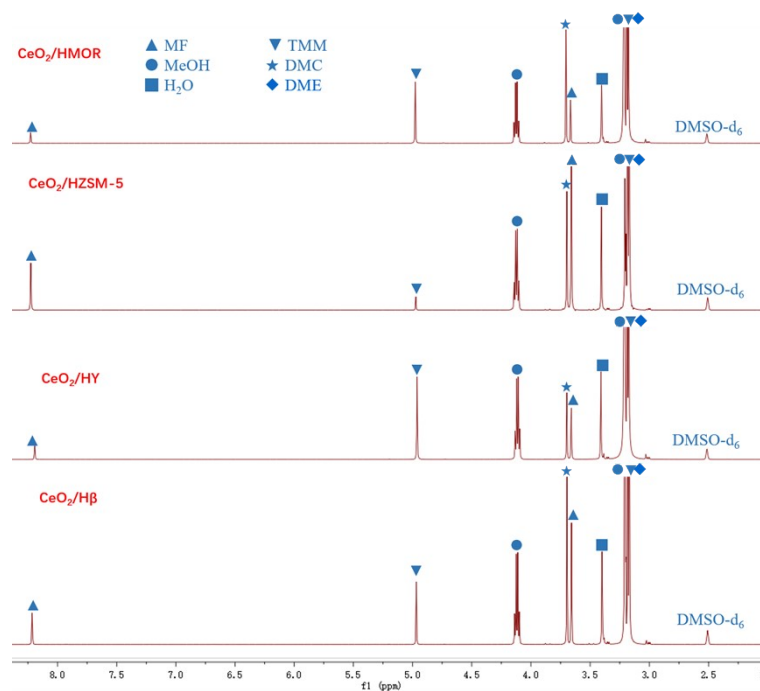


Figure S1 ^1H NMR spectra of reaction products over $\text{CeO}_2\text{-HMOR}$, $\text{CeO}_2\text{-HZSM-5}$, $\text{CeO}_2\text{-HY}$ and $\text{CeO}_2\text{-H}\beta$.

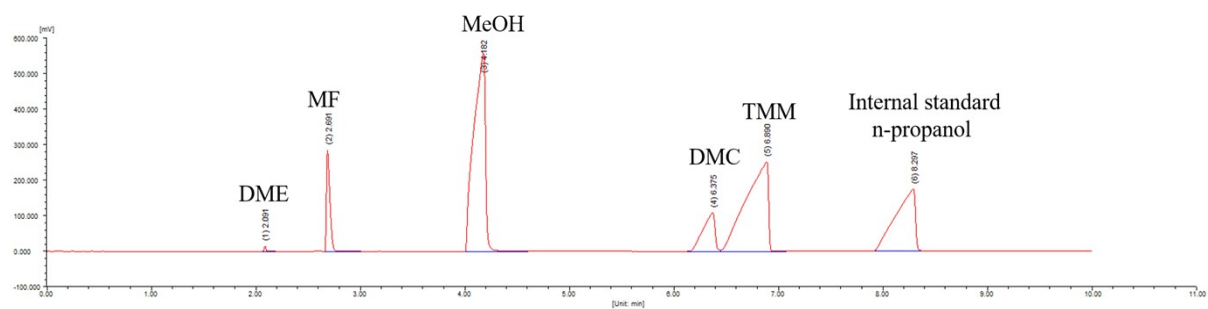


Figure S2 The gas phase chromatography signal of coproduction of dimethyl carbonate and methyl formate via CeO_2 -methanol coupling assisted by 1,1,1-trimethoxymethane hydrolysis over the CeO_2 -HMOR bicomponent catalyst

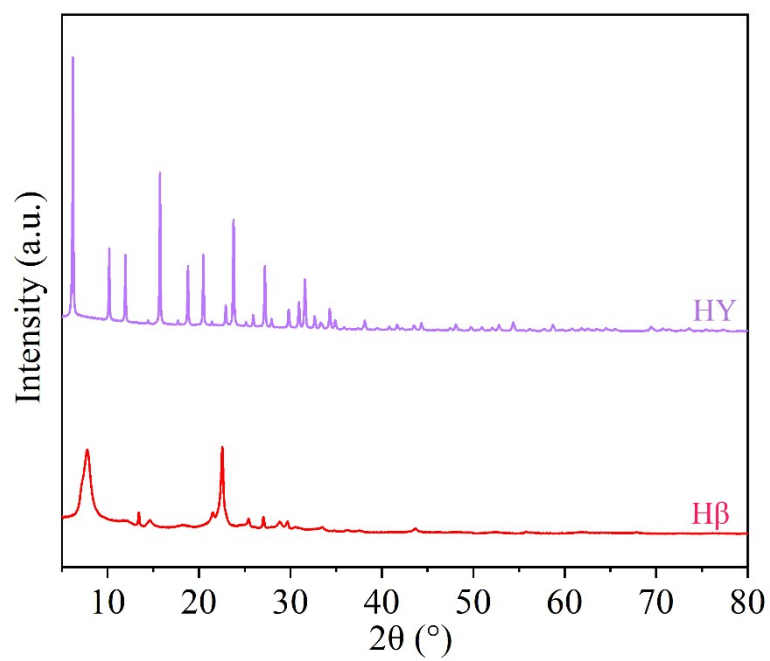


Figure S3 XRD patterns of HY and H β zeolites.

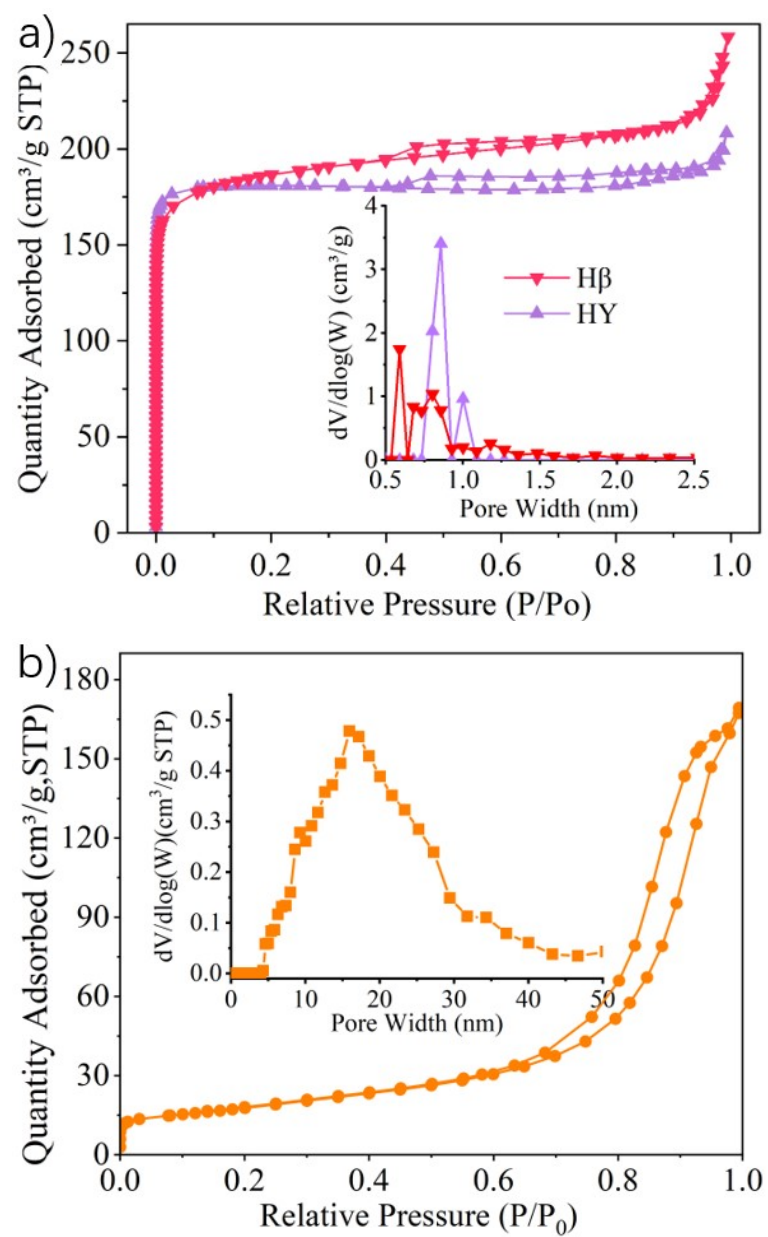


Figure S4 N_2 adsorption isotherms and pore size distributions of a) HY and H β zeolites, and b) CeO₂.

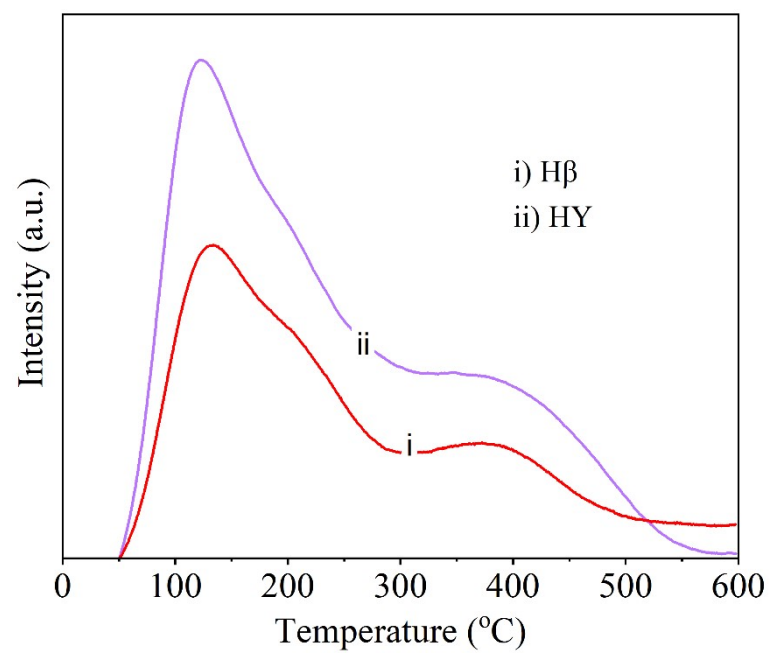


Figure S5 NH₃-TPD profiles of HY and H β .

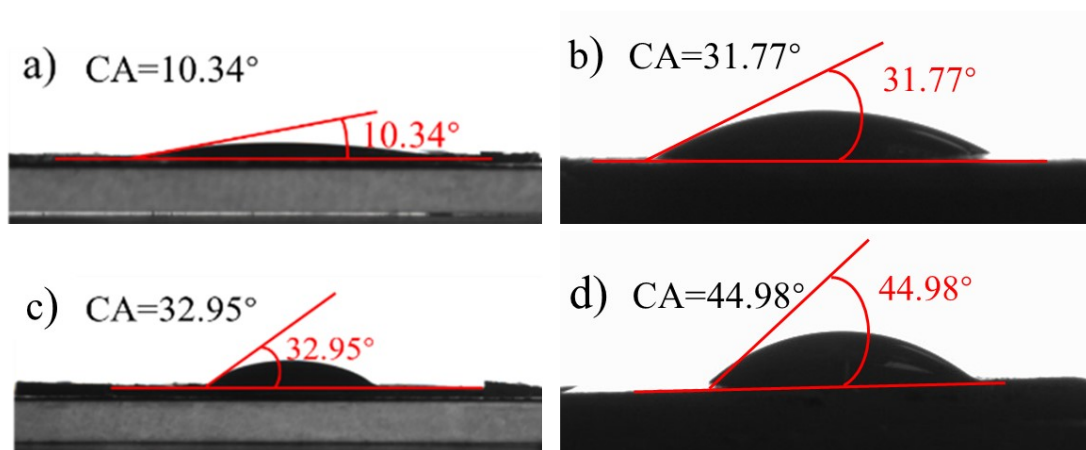


Figure S6 Contact angle of a) HMOR, b) H β , c) HZSM-5 and d) HY.

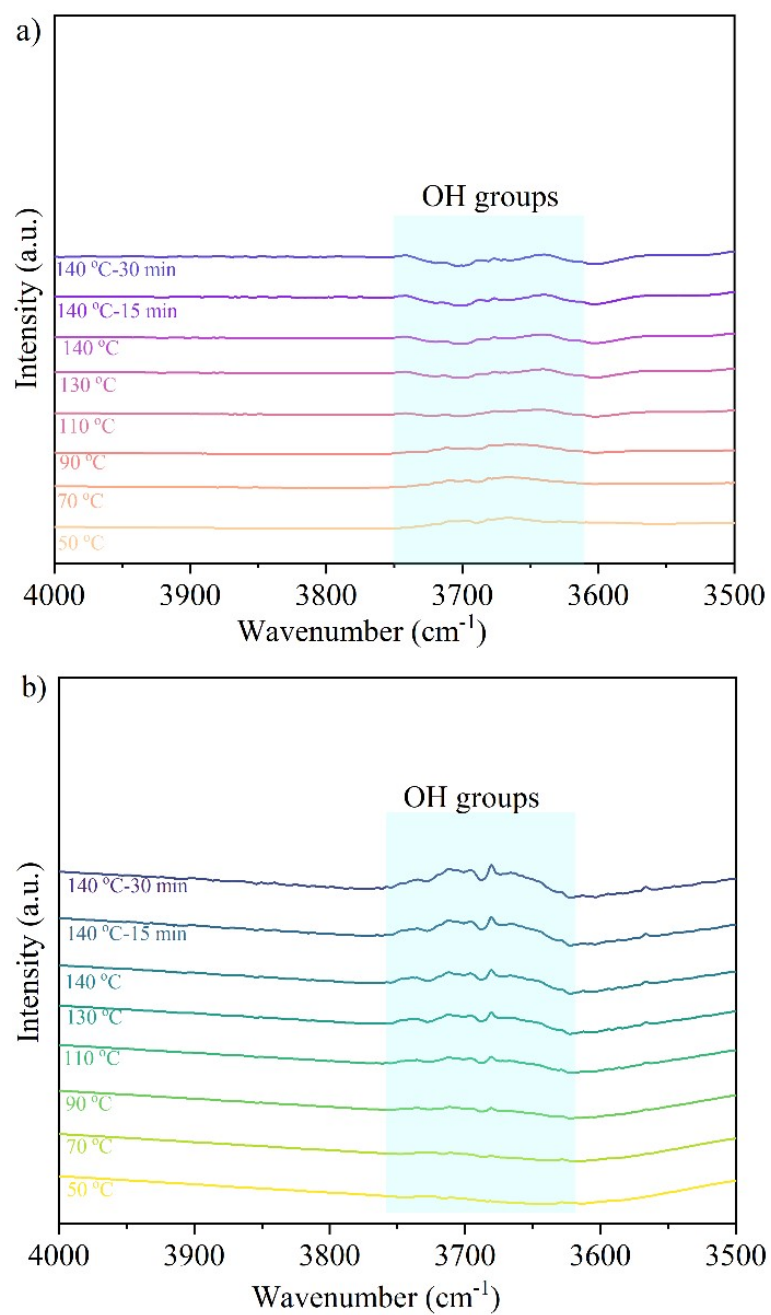


Figure S7 In-situ IR spectra in the region of 3620 – 3700 cm^{-1} wavenumber for a) CeO_2 -HMOR and b) CeO_2 after adsorption of the mixture of methanol, TMM and CO_2 .

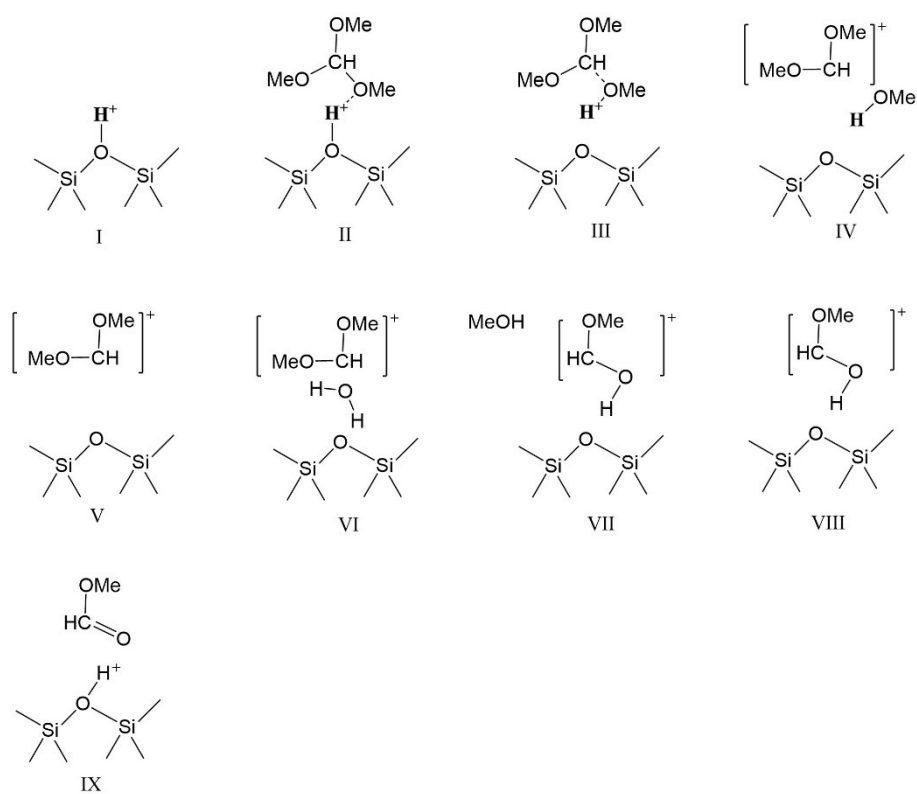


Figure S8 The detailed structure of intermediates in TMM hydrolysis reaction.

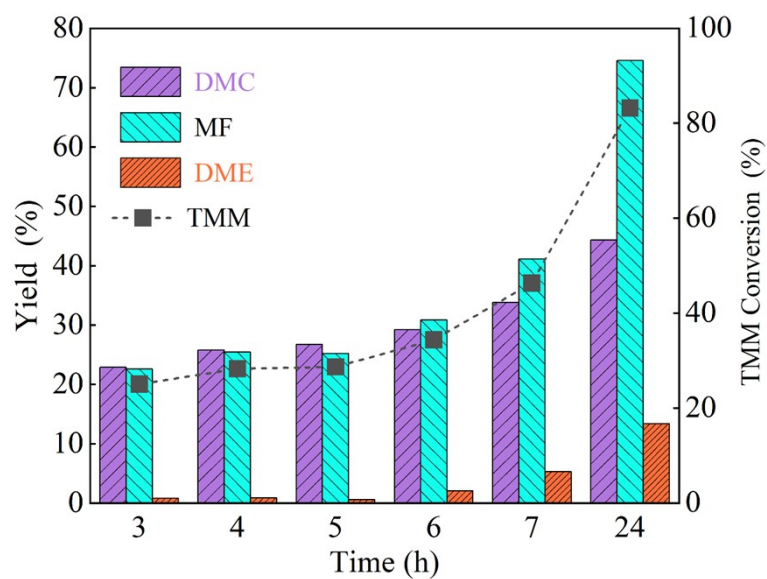


Figure S9 Effect of reaction time on catalytic performance of CeO₂-HMOR bicomponent catalyst under identical reaction conditions: $n_{\text{MeOH}}=372$ mmol, $n_{\text{TMM}}=186$ mmol, $m_{\text{CeO}_2} = 0.1$ g, $m_{\text{zeolites}} = 0.4$ g, $P_{\text{CO}_2} = 4.0$ MPa, $T_r = 140$ °C.

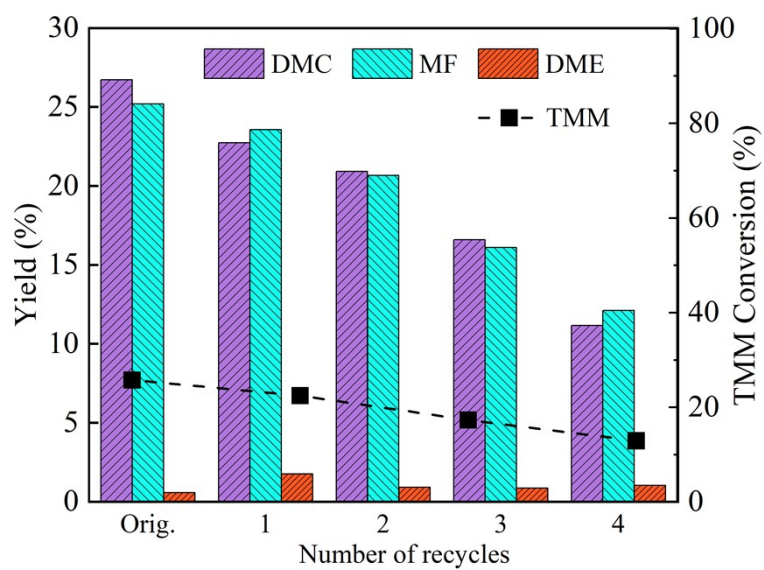


Figure S10 Recyclability tests of the CeO₂-HMOR bicomponent catalyst under identical reaction conditions. $n_{\text{MeOH}}=372$ mmol, $n_{\text{TMM}}=186$ mmol, $m_{\text{CeO}_2} = 0.1$ g, $m_{\text{HMOR}} = 0.4$ g, $P_{\text{CO}_2} = 4.0$ MPa, $T_r = 140$ °C, $t=5$ h.

Table S1. Catalytic performance for TMM hydrolysis reaction over zeolites catalysts.

Zeolites	TMM Conversion (%)	Yield (%)		
		DMC	MF	DME
HMOR	100	0	78.0	1.4
H β	100	0	74.3	0.4
HZSM-5	100	0	85.9	3.2
HY	100	0	77.3	0.3

Reaction conditions: $n_{TMM} = 186$ mmol, $n_{H_2O} = 186$ mmol, $m_{zeolites} = 0.2$ g, $P_{CO_2} = 3.0$ MPa, $T_r = 140$ °C, $t_r = 5$ h

Table S2. Characterization data of the CeO₂, HMOR, HZSM-5, H β and HY.

Catalyst	S_{BET}^a	S_{t-plot}^b	V_{total}^c	V_{t-plot}^d	SiO ₂ /Al ₂ O ₃ ^e
	(m ² g ⁻¹)	(m ² g ⁻¹)	(mL g ⁻¹)	(mL g ⁻¹)	
CeO ₂	63	9	0.25	0	/
HMOR	401	381	0.24	0.19	25
HZSM-5	303	244	0.16	0.12	27
H β	602	465	0.40	0.23	27
HY	568	557	0.32	0.28	5

^aBET surface area, ^b*t*-plot surface area, ^cTotal volume of pores at P/Po=0.99, ^d*t*-plot micropore volume, ^emolar ratio of SiO₂/Al₂O₃.

Table S3. Acid amounts determined by NH₃-TPD of the CeO₂, HMOR, HZSM-5, H β and HY zeolites.

Catalyst	Weak acid (mmol g ⁻¹)	Moderate acid (mmol g ⁻¹)	Strong acid (mmol g ⁻¹)	Total acid (mmol g ⁻¹)
CeO ₂	0.18	0.19	0.15	0.52
HMOR	0.98	0.66	0.58	2.23
HZSM-5	0.84	0.86	0.55	2.25
HY	1.51	1.27	0.42	3.20
H β	0.94	0.79	0.32	2.05

Table S4. Amounts of Lewis acid and Brønsted acid determined by *py*-IR of the HMOR and HZSM-5 zeolites.

Catalyst	Temperature (°C)	Amounts ($\mu\text{mol g}^{-1}$)		
		Lewis acid	Brønsted acid	Total acid
HMOR	150	45.9	183.3	229.2
	350	33.6	150.6	184.2
HZSM-5	150	103.1	218.2	321.3
	350	27.9	188.1	216.0

Table S5. Effect of mole ratio of MeOH/TMM on catalytic performance over CeO₂-HMOR catalysts.

Mole ratio of MeOH/TM M	TMM Conversion (%)	Yield based on MeOH (%)		Yield based on TMM (%)			DMC formation rate (mmol g _{CeO₂} ⁻¹)
		DMC	DME	DMC	MF	DME	
1	28.7	41.2	4.8	20.6	25.2	2.4	381.5
2	27.0	21.4	2.3	21.4	24.7	2.3	395.8
4	22.2	9.2	0.8	18.4	20.3	1.5	342.2

Reaction conditions: $m_{\text{CeO}_2} = 0.1$ g, $m_{\text{zeolites}} = 0.4$ g, $P_{\text{CO}_2} = 3.0$ MPa, $T_r = 140$ °C, $t_r = 5$ h

Table S6. Catalytic performance for CO₂ and H₂O coupled with TMM over the CeO₂-HMOR catalyst

Catalyst	Reactant (mmol)		TMM Conversion (%)	Yield based on TMM (%)		
	TMM	H ₂ O		DMC	MF	DME
CeO ₂ -HMOR	186	186	99.9	0.1	77.3	Trace
CeO ₂ -HMOR	186	141	87.7	9.6	64.5	0.3
CeO ₂ -HMOR	186	56	62.1	24.0	52.3	2.7
CeO ₂ -HMOR	186	0	58.2	1.1	72.7	5.8

Reaction conditions: $m_{\text{CeO}_2} = 0.1$ g, $m_{\text{HMOR}} = 0.4$ g, $P_{\text{CO}_2} = 4.0$ MPa, $Tr = 140$ °C, $tr = 5$ h

Table S7. DMC formation rate over CeO₂-HMOR compared to the excellent catalysts reported in the literature in DMC synthesis from CO₂ and methanol.

Sample	MeOH [mL]	TMM [mL]	T_r [°C]	P_{CO_2} [Mpa]	t_r [h]	DMC formation rate		Reference
						[mmol g _{CeO₂} ⁻¹]	[mmol g _{CeO₂} ⁻¹ h ⁻¹]	
CeO ₂ -HMOR	15.1	20.3	140	4	5	465.1	93.0	This work
CeO ₂ -HMOR	15.1	20.3	140	4	24	821.2	34.2	This work
ZrO ₂ -13X	1	1.3	130	2	48	61.0	1.3	[10]
CeO ₂	60	78	130	2	48	199.5	4.2	[11]
Ce ₃ -NPs/Co ₇ - NSs	3.5	5.5	120	5	12	34.8	2.9	[12]
[EMIM]Br/Ce _{0.5} Zr _{0.5} O ₂	5	4	100	12	48	13.0	0.3	[13]
HPW@MOF-808	8	10	140	12	4	9.4	2.4	[14]
MOF-808-X	8	10	140	12	4	6.4	1.6	[15]

Table S8. Acid and base amountsof the fresh and spent CeO₂-HMOR bicomponent catalyst.

Catalyst	Total acid ^a (mmol/g)	Total base ^b (mmol/g)
Fresh CeO ₂ -HMOR	1.47	0.29
Spent CeO ₂ -HMOR	0.74	0.20

^a determined by NH₃-TPD, ^b determined by CO₂-TPD,

References

- [1] Li, L.; Liu, W. X.; Chen, R. H.; et al.; Atom-economical synthesis of dimethyl carbonate from CO₂: Engineering reactive frustrated Lewis pairs on ceria with vacancy clusters. *Angewandte Chemie International Edition* **2022**, 61(51), e202214490.
- [2] VandeVondele, J.; Krack, M.; Mohamed, F.; et al.; Quickstep: Fast and accurate density functional calculations using a mixed Gaussian and plane waves approach. *Computer Physics Communications* **2005**, 167(2), 103-128.
- [3] Perdew, J.P.; Density-functional approximation for the correlation energy of the inhomogeneous electron gas. *Phys. Rev. B* **1986**, 33, 8822-8824.
- [4] Perdew, J.P.; Burke, K.; Ernzerhof, M.; Generalized gradient approximation made simple. *Phys. Rev. Lett.* **1996**, 77, 3865-3868.
- [5] Grimme, S.; Antony, J.; Ehrlich, S.; Krieg, H.; A consistent and accurate ab initio parametrization of density functional dispersion correction (DFT-D) for the 94 elements H-Pu. *J Chem Phys* **2010**, 132, 154104.
- [6] Lippert, G.; Michele, P.; Jurg, H.; A hybrid Gaussian and plane wave density functional scheme. *Mol. Phys.* **1997**, 92, 477-488.
- [7] VandeVondele, J.; Hutter, J.; Gaussian basis sets for accurate calculations on molecular systems in gas and condensed phases. *J Chem Phys* **2007**, 127, 114105.
- [8] Goedecker, S.; Teter, M.; Hutter, J.; Separable dual-space Gaussian pseudopotentials. *Phys. Rev. B* **1996**, 54, 1703.
- [9] Henkelman, G.; Jónsson, H.; Improved tangent estimate in the nudged elastic band method for finding minimum energy paths and saddle points. *J Chem Phys* **2000**, 113, 9978-9985.
- [10] Shi, D.; Heyte, S.; Capron, M.; and Paul, S.; Direct synthesis of dimethyl carbonate from methanol and CO₂ over ZrO₂ catalysts combined with a dehydrating agent and a cocatalyst. *Catalysts* **2024**, 14, 657.
- [11] Shi, D.; Heyte, S.; Capron, M.; and Paul, S.; Ceria-catalysed production of dimethyl carbonate from methanol and CO₂: effect of using a dehydrating agent combined with a solid cocatalyst. *Molecules* **2024**, 29, 5663.
- [12] He, Z.-H.; Sun Y. -C.; Wei, Y.-Y.; et al.; Synthesis of dimethyl carbonate from CO₂ and methanol over CeO₂ nanoparticles/Co₃O₄ nanosheets. *Fuel* **2022**, 325, 124945.
- [13] Zhang, Z.-F.; Liu, Z.-W.; Lu, J.; and Liu Z.-T.; Synthesis of dimethyl carbonate from carbon dioxide and methanol over Ce_xZr_{1-x}O₂ and [EMIM]Br/Ce_{0.5}Zr_{0.5}O₂. *Ind. Eng. Chem. Res.* **2011**, 50, 1981–1988.
- [14] Xuan, K.; Chen, S.; Pu Y.; et al.; Encapsulating phosphotungstic acid within metal-organic framework for direct synthesis of dimethyl carbonate from CO₂ and methanol. *Journal of CO₂ Utilization* **2022**, 59, 101960.
- [15] Xuan, K.; Pu, Y.; Li, F.; et al.; Metal-organic frameworks MOF-808-X as highly efficient catalysts for direct synthesis of dimethyl carbonate from CO₂ and methanol. *Chinese Journal of Catalysis* **2019**, 40, 553–566.